Predicting shifting sustainability tradeoffs in marine finfish aquaculture under climate change

Running head: Aquaculture management under climate change

Gianluca Sarà[1,2,*], Tarik C. Gouhier[3], Daniele Brigolin[4,5], Erika M. D. Porporato[5], M. Cristina Mangano[1,2], Simone Mirto[6], Antonio Mazzola[1,2] and Roberto Pastres[4,5]

[1]Dipartimento di Scienze della Terra e del Mare, Università degli Studi di Palermo, Viale delle Scienze Ed. 16, 90128, Palermo, Italy

[2]CoNISMa – Piazzale Flaminio, 9 – Roma, Italy

[3]Marine Science Center, Northeastern University, 430 Nahant Road, Nahant 01908

[4]Bluefarm S.r.l., Via delle Industrie 15, 30175 Venezia Marghera, Italy

[5]Dipartimento di Scienze Ambientali, Informatica e Statistica, Università Ca' Foscari Venezia, Via Torino 155, 30170 Venezia Mestre, Italy

[6]Institute for the Coastal Marine Environment – CNR, Via G. da Verrazzano 17, 91014 Castellammare del Golfo (TP), Italy

Keywords: aquaculture, mechanistic predictive models; trade-offs, regional climate models; seabass; Mediterranean Sea

Article type: Original Research – Primary Research Articles

[*]Corresponding author: gianluca.sara@unipa.it (G. Sarà)

ABSTRACT

Defining sustainability goals is a crucial but difficult task because it often involves the quantification of multiple interrelated and sometimes conflicting components. This complexity may be exacerbated by climate change, which will increase environmental vulnerability in aquaculture and potentially compromise the ability to meet the needs of a growing human population. Here, we developed an approach to inform sustainable aquaculture by quantifying spatio-temporal shifts in critical trade-offs between environmental costs and benefits using the time to reach the commercial size as a possible proxy of economic implications of aquaculture under climate change. Our results indicate that optimizing aquaculture practices by minimizing impact (this study considers as impact a benthic carbon deposition $\geq$ 1 gC m^{-2} d^{-1}) will become increasingly difficult under climate change. Moreover, an increasing temperature will produce a poleward shift in sustainability trade-offs. These findings suggest that future sustainable management strategies and plans will need to account for the effects of climate change across scales. Overall, our results highlight the importance of integrating environmental factors in order to sustainably manage critical natural resources under shifting climatic conditions.

Introduction

Sustainability is a complex, layered and inherently multidisciplinary concept that spans multiple fields including environmental science, social policy and economics, also known as the three dimensions of sustainable development (ICSU & ISSC, 2015). The environment and the services it provides represent the base layer upon which social and economic policy relies. Sustainable development, which strives to meet the needs of a growing human population while safeguarding Earth's stressed life-support systems (ICSU & ISSC, 2015), is becoming increasingly important in an era of global change and large-scale biodiversity decline (Barnosky *et al.*, 2011; Barnosky *et al.*, 2012; Cardinale *et al.*, 2012). Most national and international legislative efforts have highlighted the critical role that sustainability plays in ensuring the welfare of current and future generations.

The 2030 Agenda for Sustainable Development (ICSU & ISSC, 2015), the Sustainable Development Goals (SDGs and related targets, adopted in 2015), the Mediterranean Strategy for Sustainable Development 2016-2025 (UNEP/MAP, 2016) and the Paris Agreement of the Conference of the Parties (COP21) of the United Nations Framework Convention on Climate Change have greatly influenced and addressed the exploitation of natural resources at sea (*i.e.*, such as fishery and aquaculture) (Visbeck, 2018). Although the importance of environmental sustainability has been widely recognized and supported by integrated frameworks (Costanza *et al.*, 1997), very few attempts have been made to objectively quantify and operationally define the existing trade-offs between the three sustainability components in the aquaculture sector (Tlusty & Thorsen, 2017). Operationally defining sustainability goals under current conditions is difficult as it involves the quantification of multiple,

interrelated and often-conflicting components. The complexity of this task is expected to be exacerbated by climate change and, in particular, rising temperatures which will increase environmental vulnerability and, in applied fields such as aquaculture, will have important social and economic repercussions that are likely to extend beyond national borders. Hence, local managers and policy-makers need comprehensive credible, salient and legitimate baseline knowledge in order to quantify the environmental trade-offs to be integrated into social and economic scenarios for a sustainable development in space and time. Such information would allow the implementation of optimal ecosystem-based management strategies and strengthen the science-policy nexus (*i.e.* the relationship between environment-related science and policy FAO, 2016; Hickey *et al.*, 2013).

Aquaculture has historically focused on maximizing productivity and economic returns on very short time scales. Although such practices can yield positive outcomes in the short term, the net results in the medium to long term are often negative from a social, environmental and economic perspective. Overall, future aquaculture development needs to adopt a more integrated approach that balances social, economic and environmental objectives to ensure a sustainable harvest of natural resources over multiple time horizons (ICSU & ISSC, 2015). Here, we developed an approach to quantify spatio-temporal shifts of critical trade-offs between environmental costs and benefits using the time to reach the commercial size as a possible proxy of commercial implications of aquaculture under climate change. To forestall shifts will allow one to inform policy changes and avoid the risk for a growing disparity of responses between Mediterranean countries and societies (UNEP/MAP, 2016).

The described approach relies on predictive models based on fundamental biological characteristics of species (*i.e.*, Functional Traits [FT], *sensu* Schoener, 1986; Sarà *et al.*, 2014). At scales relevant to national management (Economic Exclusive Zones, EEZ, Figs. S1 and S2), the development of FT-based approaches (Schoener, 1986) can be used to generate the kinds of species- and site-specific mechanistic predictions of environmental costs and benefits needed to quantify trade-offs and inform sustainable development objectives (Sarà *et al*., 2018a). Such a mechanistic approach is critical for devising an optimal spatial allocation strategy that simultaneously maximizes commercial benefits (production) and minimizes environmental effects (pollution). Indeed, by quantifying how the relationship between biomass productivity and environmental impact (*i.e.*, the amount of organic loading derived from aquaculture; LOAD) of changes over space and time, our approach can be used to design future management plans that are optimal across multiple scales. On this basis, stakeholders could identify and implement proactive, site-specific management strategies tailored to target species. Once such relationship is spatially-contextualized and mapped, it represents, in practice, the quantitative informational baseline that scientists, policy makers and stakeholders need to produce management strategies and plans that will also adapt to the combined multiple pressures of climate change (Kearney & Porter, 2009; Shelton, 2014; Pacifici *et al.*, 2015; Payne *et al.*, 2015; Sarà *et al.*, 2018b).

Overall, the proposed approach will document spatio-temporal patterns of covariation between environmental cost and benefit maximized changes under current and future climate conditions and narrowing the science-policy communication gap (Hickey *et al.*, 2013). We chose the aquaculture sector as a model system to test how climate change (IPCC AR5 scenarios; 2015 *vs.* 2030 *vs.* 2050) will affect the

sustainable management of a critical natural resource. Mechanistic FT-based models are ideal in aquaculture and in most intensive terrestrial cultures (Koenigstein *et al.*, 2016) since the effects of species interactions (*e.g.*, competition for space and resource and predator-prey relationships) can be controlled *via* active management. We applied such mechanistic FT-based models on the Mediterranean seabass, *Dicentrarchus labrax* (Fig. S3). The Mediterranean seabass is an ideal model as it is one of the most traded species in the world (Sarà *et al.*, 2012) and one of the fastest-growing cultivated fish in the Mediterranean Sea (FAO, 2016). Additionally, the Mediterranean seabass may represent the candidate target for Northern Europe aquaculture, owing to expected climate-induced temperature increases in the region in future; the species has an affinity toward the future expected temperature in this area (EUMOFA, 2016).

Materials and methods

A framework (Figure 1) comprising of six steps was built, exploiting the power of the mechanistic based models Dynamic Energy Budget (the DEB; Kooijman, 2010) and FiCIM (Brigolin *et al.*, 2014) as described here below.

STEP 1 - The Dynamic Energy Budget (DEB) model

The DEB model (Fig. S3) involves a complete theoretical assessment at the whole organismal level, to link habitat features, functional traits, and life history of any living organism (Kooijman, 2010). DEB was selected for this study as a suitable model to provide a whole-organismal approach, as DEB enables one to elucidate how biologically and ecologically relevant responses depend on environmental conditions (Sarà *et al.*, 2012; Kearney *et al.*, 2010). Central to the DEB theory is the concept that

food and body temperature (BT) are the primary drivers of an individual's metabolic machinery (Sarà *et al.*, 2013). The amount of ingested energy available for biological processes is regulated within the DEB theory by the Holling's functional responses (Holling, 1959). Once food is ingested, the amount of energy that flows through the organism depends at some extent on physiological rates. As all physiological rates depends on body temperature, BT is an important driver, in particular for ectotherms, such as fish and shellfish, as their BT is close to that of their surroundings. The effect of temperature on metabolism follows the Arrhenius relationship (Kooijman, 2010), which allows one to quantify how metabolic rates change within the range of tolerance in each species; such range implicitly sets the limits of the fundamental thermal niche of a given species (Kearney & Porter, 2009).

To provide reliable predictions, the *Dicentrarchus labrax* model was implemented through a systematic review (*Mangano et al.,* 2017a) performed to deliver some preliminary parameters needed to further calibrate the *Dicentrarchus labrax* DEB model. Details about the model calibration and validation are given in the *Supporting information* section (Table S1, S2, and S3; Fig. S4). The Arrhenius formulation includes a specie-specific parameter, *i.e.* the Arrhenius temperature (TA), which, in this study, was estimated as the slope of the linear regression between the logarithm of fish oxygen consumption rate and absolute temperature. The lower and upper boundaries of the BT tolerance range were extrapolated from the literature (Dalla Via *et al.*, 1987; Claireaux & Lagardere, 1999; Person-Le Ruyet *et al.*, 2004; Claireaux & Lefrançois, 2007); these parameters are listed in Table S1. Once the DEB model was validated, the outputs were used to map the productivity index TIME (see Fig. 1) and feed the FiCIM model, as

161 described below. Details about the model calibration and validation are provided in the
162 *Supporting information* section (Model validation section and Figure S4).
163
164 **STEP 2 – FiCIM (Fish cage Integrated Model; Brigolin *et al.*, 2014)**
165 Organic matter accumulation and associated negative effects on benthic
166 communities has been identified as a key negative interaction of fish cages with the
167 surrounding marine environment (Hargrave *et al.*, 2005). Here, we simulated this
168 impact by coupling the DEB model described in STEP 1 with the particle tracking and
169 deposition modules of the FiCIM (Brigolin *et al.*, 2014). These modules allow one to
170 obtain 2D maps of elemental fluxes of organic Carbon [g C m^{-2} d^{-1}] at the water-
171 sediment interface on the basis of the amount and composition of organic matter
172 particles released by a fish farm as faeces and uneaten feed (*e.g.* Figure S5). The model
173 requires the following as input: i) time series of the amount and elemental composition
174 of uneaten feed and faeces released by fish farms; ii) time series of water currents (see
175 STEP 3); iii) bathymetry of the area in which a fish farm is located.
176 FiCIM produces output time series of fluxes of organic C, N, and P deposited on
177 the seabed surrounding a fish farm. To provide a synthetic index, the average deposition
178 of organic C was computed, named LOAD hereafter, expressed as g C m^{-2} day^{-1}, for
179 each grow-out production phase, at each grid point. Subsequently, based on Cromey *et*
180 *al.* (1998) and Hargrave *et al.* (2008), an impact threshold, *i.e.* 1 g C m^{-2} d^{-1} was set,
181 above which a grid point is classified as impacted (*i.e.* areas in which LOAD exceeds
182 the threshold).
183 The species-specific LOAD index takes into account the effects of prolonged
184 organic matter accumulation underneath a fish farm, which depletes the concentration of

185 dissolved oxygen in surface sediment, leading to changes in macrofauna community
186 structure (Cromey *et al.*, 2002; Hargrave *et al.*, 2008). LOAD was determined on a grid
187 of 5m x 5m resolution by tracking 10,000 particles per day. The parameters used in the
188 deposition module and their references are reported in Table S4**.** The initial positions of
189 faecal particles and uneaten feed pellets were randomly chosen within, respectively, the
190 volume at a fish cage and its surface. The settling velocity of each particle was
191 randomly selected from a Gaussian distribution (parameters are reported in Table S4).
192 The model was coded in Fortran and run on SCSCF (www.dais.unive.it/scscf), a
193 multiprocessor cluster system owned by Ca' Foscari University of Venice.
194
195 **STEP 3 - Estimation of input data**
196 In principle, all forcings needed to run the DEB seabass model and FiCIM
197 should be estimated for the whole study area on the basis of site-specific data; however,
198 in practice, this is not feasible, both because of the lack of a comprehensive dataset and
199 the computational effort required by the FiCIM model. Therefore, to be consistent with
200 the aim of the paper, we proceeded with the following: i) discretization of the study
201 area, ii) estimation of DEB forcing function, and iii) estimation of FiCIM forcing
202 function.
203
204 *Discretization of the study area*
205 In order to identify the study area, a 10 km coastline buffer with bathymetric
206 data and excluded areas deeper than 200 meters was clipped, which would lie outside
207 the continental shelf. The resulting study area extended along a buffer of 10 km across
208 the continental shelf of the Mediterranean and Black Sea (Fig. S6); the total surface was

209 approximately 262,395 km^2. Bathymetric data were accessed from the General
210 Bathymetric Chart of the Ocean (GEBCO_2014, http://www.gebco.net/) at 30 seconds
211 arc resolution (~1 km).
212
213 *Estimation of the DEB forcing functions*
214 As stated, DEB models require Body Temperature (BT) as input time series. To
215 apply the approach visualized in Figure 1 to the whole study area, we took the Sea
216 Surface Temperature (SST) as a proxy of BT. Time series of SST data were estimated
217 from the results of the EURO-CORDEX initiative (Jacob *et al.*, 2014; Coordinated
218 Regional Climate Downscaling Experiment). This Regional Climate Model is based on
219 the IPCC Fifth Assessment Report (AR5) CMIP5 (Coupled Model Intercomparison
220 Project). Data were downloaded (https://esgf-index1.ceda.ac.uk/projects/esgf-ceda/)
221 concerning the Representative Concentration Pathways, RCP 4.5, with a spatial
222 resolution of 0.11 degrees (~12.5 km). Next, three time series of daily SST for the
223 following years: 2012-2014, 2030-2032, and 2048-2050 were extracted, hereafter
224 labelled 2015, 2030, and 2050, respectively, and rescaled the data at 1 km, the same
225 spatial resolution of the bathymetry dataset (applying the nearest neighbour
226 interpolation) (Kotlarski *et al*., 2014).
227 The study area was partitioned into sub-regions characterized by similar annual
228 mean temperature for the three temperature scenarios. In order to obtain these sub-
229 regions, we divided the range of average temperatures for each scenario into 0.5°C
230 intervals and aggregated each grid point of the spatial domain within the resulting
231 classes; each class then included all cells falling within "Similar Average Temperature
232 Regions" (SATRs). Subsequently, we estimated an average three year SST time series

233 for each SATR to be used as input to the DEB model. SST data in NetCDF format were
234 transformed in comma-separated values (CSV) format suitable for the DEB model using
235 software developed by NASA Goddard Institute for Space Studies (Panoply; GISS,
236 http://www.giss.nasa.gov/tools/panoply/). All NetCDF files were handled using
237 Climatic Data Operators (CDO) software (1.6.4 version; Max-Planck Institut für
238 Meterologie). Daily SST values of each SATR were used to feed the DEB model as a
239 proxy of individual BT to compute the spatial distributions of the outputs of the DEB
240 model (TIME, the faeces released every hour by an individual - EJE and the hourly
241 amount of uneaten feed per individual - UNF).
242
243 *Estimation of FiCIM forcing functions*
244 DEB and FiCIM were run in sequence for every SATR for each temperature
245 scenario as follows: the first model produced the TIME index and the time series of EJE
246 and UNF, which were used in turn as input for the FiCIM model to estimate the LOAD
247 index.
248 Time series of the amount and elemental composition of uneaten feed (UNF)
249 and faeces (EJE) released by a fish farm were used to estimate daily emissions of a
250 representative fish farm with 10 meter high cylindrical cages with a diameter of 15 m,
251 assuming a stocking density of 30 individual m^3, which leads to a biomass density at
252 harvest of approximately 15 kg/m^3 (Halwart *et al.*, 2007; Trujillo *et al.*, 2012). Details
253 on the coupling among individuals, the ensemble of individuals stock in cages, and
254 deposition modules in FiCIM are reported in Brigolin *et al.* (2014). The particle
255 tracking module is computationally time-consuming and, therefore, it was not possible
256 to run as many simulations as are the cells in which the study area was divided.

Therefore, in order to find representative values of the hydrodynamic circulation and bathymetry necessary for the FiCIM models, we performed the following: *i)* determined the location of fish cages within the study area, *ii)* estimated the distributions of the bathymetric and current data, and *iii)* computed the 25th, 75th and 95th percentiles as representatives values of the two distributions. Fish cage positions (Fig. S1) were determined by means of an extensive survey carried out through Google Earth (last update June 2016) within the study area following the method described by Trujillo *et al*. (2012).

Depths at cage sites were extracted from the GEBCO dataset and the EMODnet bathymetry portal (http://www.emodnet-hydrography.eu/). Daily mean current velocity data were downloaded from the European MyOcean project for every cage in the Mediterranean Sea (Copernicus Marine Service - Ocean monitoring and forecasting service; http://www.myocean.eu/) produced by means of the NEMO Ocean model version 3.4 (Madec, 2008) on a regular grid with a spatial resolution of 1/16° (*ca.* 6-7 km) from the year 2014. Eastward and northward current velocity (m s^{-1}) data were downloaded and extracted the subset of data concerning the grid cells where the fish cages were kept. Synthetic current time series were generated, assuming that the current module and main axis were normally distributed around their 25th, 75th and 95th percentiles. Variances were set on the basis of NEMO data analysis.

The sensitivity of the environmental impact indicator, LOAD, with respect to oceanographic conditions, was explored for the three percentiles considered (25th, 75th and 95th) by combining the three representative depths (11.8 m, hereafter coded as -12 m; 19.0 m and 43.6 m, hereafter coded as -44 m) with the three representative current

280 velocities (1.18 cm/s, 4.94 cm/s and 12.47 cm/s), thus obtaining 9 oceanographic
281 scenarios (see Table S5).
282
283 **STEP 4 - Mapping of model outputs**
284 We ran the modelling system for each SATR using the forcing time series
285 estimated as described previously for the 3 temperature scenarios (2015, 2030 and
286 2050) as input. Each simulation was run until an individual reached the standard
287 commercial size of 500 g according to FAO statistics
288 (http://www.fao.org/fishery/culturedspecies/Dicentrarchus_labrax/en). Finally, the two
289 indices (TIME and LOAD) for each time period were mapped (Figures S7).
290
291 **STEP 5 – Optimization trade-off**
292 *Modelling the trade-off*
293 We used 1-3 degree polynomial regressions to quantify the trade-off between the
294 environmental costs (area in m^2: LOAD) and benefits (time to reach commercial size,
295 days: TIME) impact of aquaculture for each oceanographic scenario (current speeds of
296 1.18 cm s^{-1}, 4.94 cm s^{-1} and 12.47 cm s^{-1}) and year (2015, 2030 and 2050). We then
297 used information theory (Corrected Akaike's Information Criterion, AICC) to select the
298 model with the optimal polynomial degree. In all cases, the second-degree polynomial
299 model was selected to describe the relationship between environmental and commercial
300 impacts of aquaculture as an inverted parabola. The ascending section of the parabola
301 represented a positive correlation between environmental and commercial components
302 (no trade-off), whereas the descending section represented a negative correlation
303 between environmental and commercial components (trade-off). Values found in the

ascending section were color-coded in red (no trade-off), whereas those found in the descending section were color-coded in blue (trade-off) (Fig. S8).

Commercial-to-environmental impact sensitivity analysis

An extensive sensitivity analysis was conducted to determine how the trade-off changed under different assumptions regarding the relative valuation of commercial and environmental components for each oceanographic scenario and year. To do so, we computed the z-scores of the commercial (z_C) and environmental (z_E) components by subtracting the mean from each value and dividing by the standard deviation. These dimensionless z-scores thus measure the "distance" between each component value and its mean in terms of the number of standard deviations; hence, z-scores that are negative lie below the mean and *vice versa*. We then computed the total impact as $z_{total} = z_C + a\ z_E$, where "a" represents a scalar used to alter the relative weight of commercial and environmental components on total impact. We further explored values ranging from 0 to 5 to determine the robustness of our results to different weightings of commercial and environmental components.

STEP 6 – Optimization spatial mapping

Optimization maps were produced joining the results obtained from the analysis carried out in STEP 5 with each SATR, both no trade-off and trade-off SATRs were represented. No trade-off indicates the regions where a reduction in TIME should also reduce the environmental LOAD and *vice versa*, while at the trade-off regions a reduction in TIME should increase the environmental LOAD and *vice versa*. Fig. S9

327 shows the difference in impacted areas between the 2015 and 2050 scenarios and
328 between the 2030 and the 2050 scenarios.
329
330 **Results**
331 Our findings show that increasing temperatures under climate change will
332 positively affect the time-to-reach commercial size (TIME, in days) according to a
333 latitudinal gradient (Figure 2).
334 In particular, most areas will have an increase in TIME between 2015 (days =
335 939) *vs.* 2030 (days = 956), whereas between 2015 and 2050 (days = 937), the length of
336 coastline where the TIME will be shorter, will increase. The environmental impact of
337 aquaculture (LOAD) was quantified by measuring the amount of total coastline area
338 (m^2) affected by produced ejections (EJE) and uneaten feed (UNF) under multiple
339 oceanographic conditions (intermediate oceanographic conditions shown in Figure 3;
340 other conditions shown in Table S5). The areas with increasing LOAD will increase
341 between 2015 and future scenarios (Figure 3) with a heterogeneous spatial pattern
342 (Figure S7).
343 In general, these maps show that the spatial distributions of commercial and
344 environmental changes will vary in complex ways over time. To determine the
345 relationship between commercial and environmental changes as well as their covariation
346 in space and time, we regressed the environmental against the commercial components
347 using second-degree polynomials for each oceanographic scenario and year. Our
348 analyses among the three oceanographic scenarios showed a unimodal relationship
349 between environmental and commercial components (inverted parabola), with

environmental and commercial components positively correlated in the ascending region and negatively correlated in the descending region (Figure 4).

In the ascending region, there was no trade-off between environmental and commercial components, as reducing either would reduce the overall climate change effect. Conversely, in the descending region, there was a trade-off between environmental and commercial components, as reducing one would not necessarily reduce the overall impact. There appears to be a strong latitudinal signal in the distribution of the trade-off between commercial and environmental components across all oceanographic scenarios in 2015, with northern regions being dominated by a tradeoff and southern regions by a lack of trade-off (Figure 5). However, this latitudinal signal decayed over time across all oceanographic scenarios, as tradeoff and no-tradeoff regions become more interspersed in space (Figure 5). Additionally, although the first two oceanographic scenarios indicate a southern expansion of the trade-off regions, the third oceanographic scenario indicates a northern expansion of the no trade-off regions (Figure 5).

Although quantifying the commercial and environmental components of climate change separately across the Mediterranean Sea is an important first step, stakeholders require an integrated metric in order to facilitate spatial planning and management of aquaculture activities. We devised a measure of total impact (z_{total}) by summing z-scores of the commercial (z_C) and environmental (z_E) components: $z_{\text{total}} = z_C + a\, z_E$ (see *Supporting information*). Given the lack of information regarding the relative importance or valuation of commercial and environmental impacts, we then conducted an extensive sensitivity analysis to determine how different weightings of these two components would affect the total impact of climate change by varying the value of "a,"

a measure of commercial-to-environmental impact, from 0 to 5. Our sensitivity analysis revealed that the total impact of climate change on aquaculture is expected to increase over time across all oceanographic scenarios (Figure 4). Indeed, across all three oceanographic scenarios, the total impact increased over time for all commercial-to-environmental ratios. By 2050, only regions characterized by very low values of commercial component or very low commercial-to-environmental impact ratios would be characterized by low total impacts. Most of the regions, however, were characterized by intermediate to high total impact, depending on the commercial-to-environmental ratio (Figure 4). Hence, climate change will make the practice of aquaculture challenging by increasing both the frequency of trade-offs between commercial and environmental components across the Mediterranean and Black Sea and the total impact under most valuation scenarios (Figures 4, 5, S8, and S9).

Overall, our results demonstrated that adopting an integrated framework that involve both environmental costs and benefits is necessary to anticipate vulnerabilities, reduce the risk of mismanagement and ensure the sustainability of human activities at sea under future climatic projections (Cochrane *et al.*, 2009). Present results also suggest that optimizing aquaculture practices by minimizing total impact will become increasingly difficult under climate change for most oceanographic scenarios (Table S5). Although we believe that the approach adopted and summarized in Figure 1 is sound, it is important to acknowledge that our findings should be interpreted with caution, as both the computational burden and the availability of site specific data have set some limitations to its implementation in the study area.

The index LOAD is computationally much more expensive than TIME, as it requires the integration via Montecarlo simulation of the trajectories of 7×10^9 particles

in a 2D domain, which took approximately 126 hours on the available computational resource. Therefore, it would not be easy to run FiCIM at each grid point in order to assess a site-specific impact. Furthermore, such an approach requires site-specific hydrodynamic circulation data, although data from operational oceanography could have served the purpose for 2015 scenarios, projecting currents for the 2030 and 2050 would have been highly speculative. For this reason, we explored nine oceanographic scenarios, which are representative of the present current and depth distributions of fish farms. The results of our investigation (see also the *Supporting information* section), showed that both bathymetry and average current speed play a significant role in determining the actual impact. Furthermore, our findings also show (see Figure 4) that, in most SATRs, impact decreases as TIME increases, such that wherever an increase in temperature will shorten the grow-out phase, one can expect an increase in the moderately impacted benthic area. To this regard, we would like to point out that this area was defined on the basis of a threshold suggested by the literature, *i.e.* 1 g C m^{-1} d^{-1} (see also the *Supporting information* section), in keeping with a precautionary principle. In general, in presence of similar local bathymetry, the higher the current speed, the larger the areas affected by moderate organic enrichment, although the cumulative value of organic material deposited *per* unit surface will decrease. On the other hand, at sites characterized by low hydrodynamic dispersion this area would shrink, but the deposition of organic matter in surface could reach much higher values, inducing a shift toward anaerobic degradation pathways. Therefore, proper site selection, based on site-specific data, will become even more relevant in the future. In the present study, we did not consider the effect of an increasing temperature on the degradation of the organic matter in surface sediment, which could further increase the impact on sediment

422 biogeochemistry and, in particular, on the oxygen sediment demand. Therefore, the
423 organic carbon flux, which was taken as an indicator of moderate impact, may have to
424 be revised and likely lowered.
425
426 **Discussion**
427 This study demonstrated how climate change could cause detrimental effects on
428 sustainability when TIME and LOAD are integrated as trade-off into the environmental
429 component of sustainability. Here, the use of TIME or LOAD as sole indicators could
430 lead to counterproductive management decisions and yield net negative results (Figures
431 2 and 3) (e.g. Sea-Level-Rise in wetland systems; Kirwan & Megonigal, 2013).
432 Consistent with previous work (Poloczanska *et al.*, 2013; Rutterford *et al.*, 2015), our
433 analysis showed that increasing temperatures due to climate change would produce a
434 mean poleward shift in the environmental trade-offs. Additionally, the integration of
435 these two drivers (TIME and LOAD) of aquaculture components (environmental cost
436 and benefits) and downscaling to local conditions (*e.g.* current velocity) revealed strong
437 differences in the spatial distribution of the trade-offs over time, with spatial variability
438 increasing over time from 2015 to 2050. Since the Mediterranean and Black Sea
439 Exclusive Economic Zones (EEZs) will experience distinct trade-offs in space and time
440 (Figs. S8 and S9), management strategies must be local and adaptive in order to
441 minimize total impact (FAO, 2016). Such spatially explicit and multi-pronged
442 information is critical to develop, promote and encourage for cooperation between
443 knowledge producers (scientists) and knowledge users (policy-makers) representing a
444 solid knowledge baseline in order to tailor future effective local sustainable
445 management measures in aquaculture-dependent countries.

To this regard, the approach here proposed could be used in an adaptive management framework, with innovation in cage management aimed at lowering its environmental impact and improving its performances can be easily taken into account by changing model parameters, with respect to the estimates used in the present application. For example, as regard feed performance and feeding management (e.g. lower FCR and differences in feed elemental composition) can be accounted for by adjusting the parameters reported in Table S3, while higher buoyancy by decreasing the settling velocity of feed particles, parameter w_{fo} in Table S4.

Therefore, present approach can provide a sound environmental baseline for constructing integrated models which allows one to explore socio-economic future scenarios of i) the industry development, ii) the markets' prices adaptive replies to the climate change iii) the growing seafood proteins demands. This will allow to build proactive models for a sustainable aquaculture (Chavanne *et al.* 2016; Sarà *et al.,* 2018a).

Thus, policy and management measures must be addressed with spatial and temporal scales matching the values and issues of concern as suggested for other human activities (Muñoz *et al.*, 2015; Paterson *et al.*, 2015); however, they are only rarely applied (Creighton *et al.*, 2016; Lu *et al.*, 2015).

Although our analysis focused on a single species, this mechanistic approach can easily be extended to other aquaculture species, as it exploits the power of species-specific biological traits (*sensu* Courchamp *et al.*, 2015). Extending our framework to other species would help generate predictions about the distribution of multispecies trade-offs in space and time as well as identify winners vs. losers in the face of climate change. The generation of freely available and updated multispecies trade-off maps will

470 represent an useful tool to help researchers track progress in plugging knowledge gaps
471 and drive decision-makers, stakeholders and public opinion in developing adaptation
472 and mitigation solutions at biologically-relevant spatio-temporal scales. The seabass is
473 thought to be the best candidate for Northern Europe aquaculture although there are no
474 biological-trait databases to date to corroborate it; this remains more a working rather
475 than data-driven hypothesis.

476 Aquaculture is expected to become potentially crucial in meeting the world's
477 seafood demand since catches of most wild commercial fisheries are at or beyond their
478 maximum sustainable yield (ICSU & ISSC, 2015, FAO, 2016) with consequent
479 alteration of seabed integrity (Mangano *et al.,* 2017b). However, our analysis shows that
480 climate change may fundamentally limit the ability of aquaculture to satisfy the future
481 seafood needs of a growing human population.

482

483 **Acknowledgements**

484 PRIN TETRIS 2010 grant n. 2010PBMAXP_003, funded by the Italian Minister of
485 Research and University (MIUR), supported this research. TCG was supported by
486 grants from the US National Science Foundation (CCF-1442728, OCE-1458150). We
487 thank Dr. Alessandro Rinaldi for his help in DEB modeling effort.

488

489 **Author contributions**: G.S., T.C.G., M.C.M. and R.P. conceived the idea, addressed
490 the objective of analyses and equally led the writing; G.S., S.M., A.M., R.P. provided
491 funds, hardware and software facilities; G.S. carried out the DEB predictive modelling,
492 D.B. carried out the FICIM modelling, E.M.D.P. carried out the mapping activity;
493 M.C.M. performed the systematic review of literature.
494

495 **References**

496 Barnosky, A.D., Matzke, N., Tomiya, S., Wogan, G.O., Swartz, B., Quental, T.B.,
497 Marshall, C., McGuire, J.L., Lindsey, E.L., Maguire, K.C. & Mersey, B. (2011). Has
498 the Earth/'s sixth mass extinction already arrived?. Nature, 471(7336), pp.51-57.
499 Barnosky, A.D., Hadly, E.A., Bascompte, J., Berlow, E.L., Brown, J.H., Fortelius, M.,
500 Getz, W.M., Harte, J., Hastings, A., Marquet, P.A. & Martinez, N.D. (2012).
501 Approaching a state shift in Earth/'s biosphere. Nature, 486(7401), pp.52-58.
502 Brigolin, D., Meccia, V.L., Venier, C., Tomassetti, P., Porrello, S. & Pastres, R. (2014).
503 Modelling biogeochemical fluxes across a Mediterranean fish cage farm. Aquaculture
504 Environment Interactions, 5(1), pp.71-88.
505 Cardinale, B.J., Duffy, J.E., Gonzalez, A., Hooper, D.U., Perrings, C., Venail, P.,
506 Narwani, A., Mace, G.M., Tilman, D., Wardle, D.A. & Kinzig, A.P. (2012).
507 Biodiversity loss and its impact on humanity. Nature, 486(7401), pp.59-67.
508 Chavanne, H., Janssen, K., Hofherr, J., Contini, F., Haffray, P., Aquatrace Consortium,
509 Komen, H., Nielsen, E.E., Bargelloni, L. (2016). A comprehensive survey on selective
510 breeding programs and seed market in the European aquaculture fish industry.
511 Aquaculture International 24: 1287-1307.
512 Claireaux, G. & Lagardère, J.P. (1999). Influence of temperature, oxygen and salinity
513 on the metabolism of the European sea bass. Journal of Sea Research, 42(2), pp.157-
514 168.
515 Claireaux, G. & Lefrançois, C. (2007). Linking environmental variability and fish
516 performance: integration through the concept of scope for activity. Philosophical
517 Transactions of the Royal Society of London B: Biological Sciences, 362(1487),
518 pp.2031-2041.

519 Cochrane, K., De Young, C., Soto, D. & Bahri, T., (2009). Climate change implications
520 for fisheries and aquaculture. FAO Fisheries and aquaculture technical paper, 530,
521 p.212.
522 Costanza, R., d'Arge, R., De Groot, R., Farber, S., Grasso, M., Hannon, B., Limburg,
523 K., Naeem, S., O'neill, R.V., Paruelo, J. & Raskin, R.G. (1997). *Nature* **387**, 253-260.
524 Courchamp, F., Dunne, J.A., Le Maho, Y., May, R.M., Thébaud, C. & Hochberg, M.E.,
525 (2015). Fundamental ecology is fundamental. Trends in ecology & evolution, 30(1),
526 pp.9-16.
527 Creighton, C., Hobday, A.J., Lockwood, M. & Pecl, G.T. (2016). Adapting
528 management of marine environments to a changing climate: a checklist to guide reform
529 and assess progress. Ecosystems, 19(2), pp.187-219.
530 Cromey, C.J., Black, K.D., Edwards, A. & Jack, I.A. (1998). Modelling the deposition
531 and biological effects of organic carbon from marine sewage discharges. Estuarine,
532 Coastal and Shelf Science, 47(3), pp.295-308.
533 Cromey CJ, Nickell TD, Black KD (2002) DEPOMOD—modelling the deposition and
534 biological effects of waste solids from marine cage farms. Aquaculture 214, 211−239.
535 Dalla Via, G.J., Tappeiner, U. & Bitterlich, G. (1987). Shore-level related
536 morphological and physiological variations in the mussel *Mytilus galloprovincialis*
537 (Lamarck, 1819) (Mollusca Bivalvia) in the north Adriatic Sea. Monitore Zoologico
538 Italiano 21, 293-305.
539 EUMOFA (2016). European Market Observatory For Fisheries And Aquaculture
540 Products Monthly Highlights, N. 6/2016.
541 FAO (2016). The State Of World Fisheries And Aquaculture 2016. Contributing To
542 Food Security And Nutrition For All. Rome. 200 pp.

Halwart, M., Soto, D. & Arthur, J.R. (2007). Cage Aquaculture: Regional Reviews and Global Overview. FAO, Rome.

Hargrave, B.T. (2005). Environmental effects of marine finfish aquaculture. Handbook of Environmental Chemistry, Vol 5. Springer-Verlag, Heidelberg, 467 pp.

Hargrave, B.T., Holmer, M. & Newcombe, C.P. (2008). Towards a classification of organic enrichment in marine sediments based on biogeochemical indicators. Marine Pollution Bulletin 56, 810-824.

Hickey, G.M., Forest, P., Sandall, J.L., Lalor, B.M., & Keenan, R.J. (2013). Managing the environmental science–policy nexus in government: Perspectives from public servants in Canada and Australia. Science and Public Policy, sct004.

Holling, C.S. (1959). The components of predation as revealed by a study of small mammal predation of the European pine sawfly. The Canadian Entomologist 91, 293-320.

ICSU, ISSC (2015). Review of the Sustainable Development Goals: The Science Perspective. Paris: International Council for Science.

Jacob, D., Petersen, J., Eggert, B., Alias, A., Christensen, O.B., Bouwer, L.M., Braun, A., Colette, A., Déqué, M., Georgievski, G. & Georgopoulou, E. (2014). EURO-CORDEX: new high-resolution climate change projections for European impact research. Regional Environmental Change, 14(2), pp.563-578.

Kearney, M. & Porter, W. (2009). Mechanistic niche modelling: combining physiological and spatial data to predict species' ranges. Ecology Letters 12, 334-350.

Kearney, M., Simpson, S.J., Raubenheimer, D. & Helmuth, B. (2010). Modelling the ecological niche from functional traits. Philosophical Transactions of the Royal Society of London B: Biological Sciences, 365(1557), pp.3469-3483.

Mangano, M. C., Sarà, G., & Corsolini, S. (2017a). Monitoring of persistent organic pollutants in the polar regions: knowledge gaps & gluts through evidence mapping. Chemosphere, 172, 37-45.

Mangano, M.C., Bottari, T., Caridi, F., Porporato, E.M.D., Rinelli, P., Spanò, N., Johnson, M. and Sarà, G. (2017b). The effectiveness of fish feeding behaviour in mirroring trawling-induced patterns. Marine Environmental Research 131: 195-204.

Kirwan, M. L. & Megonigal, J. P. (2013). Tidal wetland stability in the face of human impacts and sea-level rise. Nature 504(7478), 53-60.

Koenigstein, S., Mark, F.C., Gößling-Reisemann, S., Reuter, H., & Poertner, H.O. (2016). Modelling climate change impacts on marine fish populations: process-based integration of ocean warming, acidification and other environmental drivers. *Fish Fish* DOI: 10.1111/faf.12155.

Kooijman, S.A.L.M. (2010). Dynamic Energy Budget Theory for Metabolic Organisation, 3rd edn. Cambridge University Press, Cambridge: 508pp.

Kotlarski, S., Keuler, K., Christensen, O.B., Colette, A., Déqué, M., Gobiet, A., Goergen, K., Jacob, D., Lüthi, D., van Meijgaard, E. & Nikulin, G. (2014). Regional climate modeling on European scales: a joint standard evaluation of the EURO-CORDEX RCM ensemble. Geoscientific Model Development, 7(4), pp.1297-1333.

Lu, Y., Nakicenovic, N., Visbeck, M. & Stevance, A.S. (2015). Five priorities for the UN sustainable development goals. *Nature* **521**(7550), 28-28 (2015).

Madec, G. (2008). NEMO ocean engine. Note du Pôle de modélisation, Institut Pierre-Simon Laplace (IPSL), France, No 27, ISSN No 1288-1619.

Muñoz, N. J., Farrell, A. P., Heath, J. W., & Neff, B. D. (2015). Adaptive potential of a Pacific salmon challenged by climate change. Nature Climate Change 5(2), 163-166.

591 Pacifici, M., Foden, W.B., Visconti, P., Watson, J.E., Butchart, S.H., Kovacs, K.M.,
592 Scheffers, B.R., Hole, D.G., Martin, T.G., Akçakaya, H.R. & Corlett, R.T. (2015).
593 Assessing species vulnerability to climate change. Nature Climate Change, 5(3),
594 pp.215-224.
595 Payne, M.R., Barange, M., Cheung, W.W., MacKenzie, B.R., Batchelder, H.P.,
596 Cormon, X., Eddy, T.D., Fernandes, J.A., Hollowed, A.B., Jones, M.C. & Link, J.S.,
597 (2015). Uncertainties in projecting climate-change impacts in marine ecosystems. ICES
598 Journal of Marine Science: Journal du Conseil, p.fsv231.
599 Paterson, R. R. M., Kumar, L., Taylor, S., & Lima, N. (2015). Future climate effects on
600 suitability for growth of oil palms in Malaysia and Indonesia. Scientific Reports, 5.
601 Person-Le Ruyet, J., Mahé, K., Le Bayon, N. & Le Delliou, H. (2004). Effects of
602 temperature on growth and metabolism in a Mediterranean population of European sea
603 bass, *Dicentrarchus labrax*. Aquaculture 237, 269-280.
604 Poloczanska, E.S., Brown, C.J., Sydeman, W.J., Kiessling, W., Schoeman, D.S., Moore,
605 P.J., Brander, K., Bruno, J.F., Buckley, L.B., Burrows, M.T. & Duarte, C.M. (2013).
606 Global imprint of climate change on marine life. Nature Climate Change, 3(10), pp.919-
607 925.
608 Rutterford, L.A., Simpson, S.D., Jennings, S., Johnson, M.P., Blanchard, J.L., Schön,
609 P.J., Sims, D.W., Tinker, J. & Genner, M.J. (2015). Future fish distributions constrained
610 by depth in warming seas. Nature Climate Change, 5(6), pp.569-573.
611 Sarà, G., Reid, G.K., Rinaldi, A., Palmeri, V., Troell, M. & Kooijman, S.A.L.M. (2012).
612 Growth and reproductive simulation of candidate shellfish species at fish cages in the
613 Southern Mediterranean: Dynamic Energy Budget (DEB) modelling for integrated
614 multi-trophic aquaculture. Aquaculture, 324, pp.259-266.

Sarà, G., Palmeri, V., Montalto, V., Rinaldi, A. & Widdows, J. (2013). Parameterisation of bivalve functional traits for mechanistic eco-physiological dynamic energy budget (DEB) models. Marine Ecology Progress Series, 480, pp.99-117.

Sarà, G., Rinaldi, A. & Montalto, V. (2014). Thinking beyond organism energy use: a trait-based bioenergetic mechanistic approach for predictions of life history traits in marine organisms. Marine Ecology, 35(4), pp.506-515.

Sarà, G., Mangano, M.C., Johnson, M., & Mazzola, A. (2018a). Integrating multiple stressors in aquaculture to build the blue growth in a changing sea. Hydrobiologia, 809(1), pp. 5-17.

Sarà, G., Porporato, E., Mangano, M.C., & Mieszkowska, N. (2018b). Multiple stressors facilitate the spread of a non□indigenous bivalve in the Mediterranean Sea. Journal of Biogeography. https://doi.org/10.1111/jbi.13184

Schoener, T.W. (1986). Mechanistic approaches to community ecology: a new reductionism?. American Zoologist, pp.81-106.

Shelton, C. (2014). FAO *Fisheries and Aquaculture Circular No*. 1088. Rome, FAO. 34 pp.

Tlusty, M.F. & Thorsen, Ø. (2017). Claiming seafood is 'sustainable' risks limiting improvements. Fish Fish 18, 340–346. DOI: 10.1111/faf.12170.

UNEP/MAP (2016). Mediterranean Strategy for Sustainable Development 2016-2025. Valbonne. Plan Bleu, Regional Activity Centre.

Visbeck, M. (2018). Ocean science research is key for a sustainable future. Nature communications, 9(1), 690.

Trujillo, P., Piroddi, C. & Jacquet, J. (2012). Fish Farms at Sea: The Ground Truth from Google Earth. PLoS ONE 7(2), e30546. doi: 10.1371/journal.pone.0030546.

Figures captions

Figure 1. Six-step framework based on mechanistic models (DEB and FiCIM) used to obtain mechanistic-based spatial explicit optimization.

Figure 2. The time in days required to reach commercial size, from top to the bottom, respectively, across 2015, 2030 and 2050. Nine-day classes are reported (differences in the first class are to highlight, respectively: 2015 = 587 - 600; 2030 = 593 - 600; 2050 = --; other classes include 601 - 650, 651 - 700, 701 - 750, 751 - 800, 801 - 850, 851 - 900, 901 - 950, 951 - 975). Each histogram on the left side of the panel shows the number of km^2 within each class for each examined period.

Figure 3. The impacted area (m^2; LOAD), from top to bottom, respectively, across 2015, 2030, and 2050. Five classes of impact are reported, respectively, in 2015: 16,125 - 20,000; 20,001 - 21,000; 21,001 - 22,000; 22,001 - 23,000; 23,001 - 23,750; in 2030: 17,075 - 20,000; 20,001 - 21,000; 21,001 - 22,000; 22,001 - 23,000; 23,001 - 23,650; in 2050: 17,675 - 20,000; 20,001 - 21,000; 21,001 - 22,000; 22,001 - 23,000; 23,001 - 23,575. Each histogram on the left side of the panel shows the number of km^2 within each impact class.

Figure 4. Optimization curves (upper panel). The optimization between environmental impacted area (m^2; LOAD) and time to reach commercial size (days; TIME) with Similar Average Temperature Regions (SATRs) under three different scenarios of current velocity (a = 1.18 cm/s, b = 4.94 cm/s, c = 12.47 cm/s). SATRs under a "no trade-off" condition are reported in red, SATRs in a "trade-off" condition are in blue. Different symbols refer to SATRs of each of the three time periods: circle = 2015, square = 2030, diamond = 2050. The model fits are coded based on year: solid line =

2014, dashed line = 2030, dotted line = 2050. Lower panel shows optimization trends among the three scenarios of current velocity and years 2015, 2030 and 2050.

Figure 5. Optimization maps of the Mediterranean and Black Sea across three scenarios of current velocity (scenario 1: 1.18 cm/s; scenario 2: 4.94 cm/s; scenario 3: 12.47 cm/s) and years 2015, 2030 and 2050. Blue and red bars refer to the percentage of km^2 respectively under "trade-off" or "no trade-off" conditions.

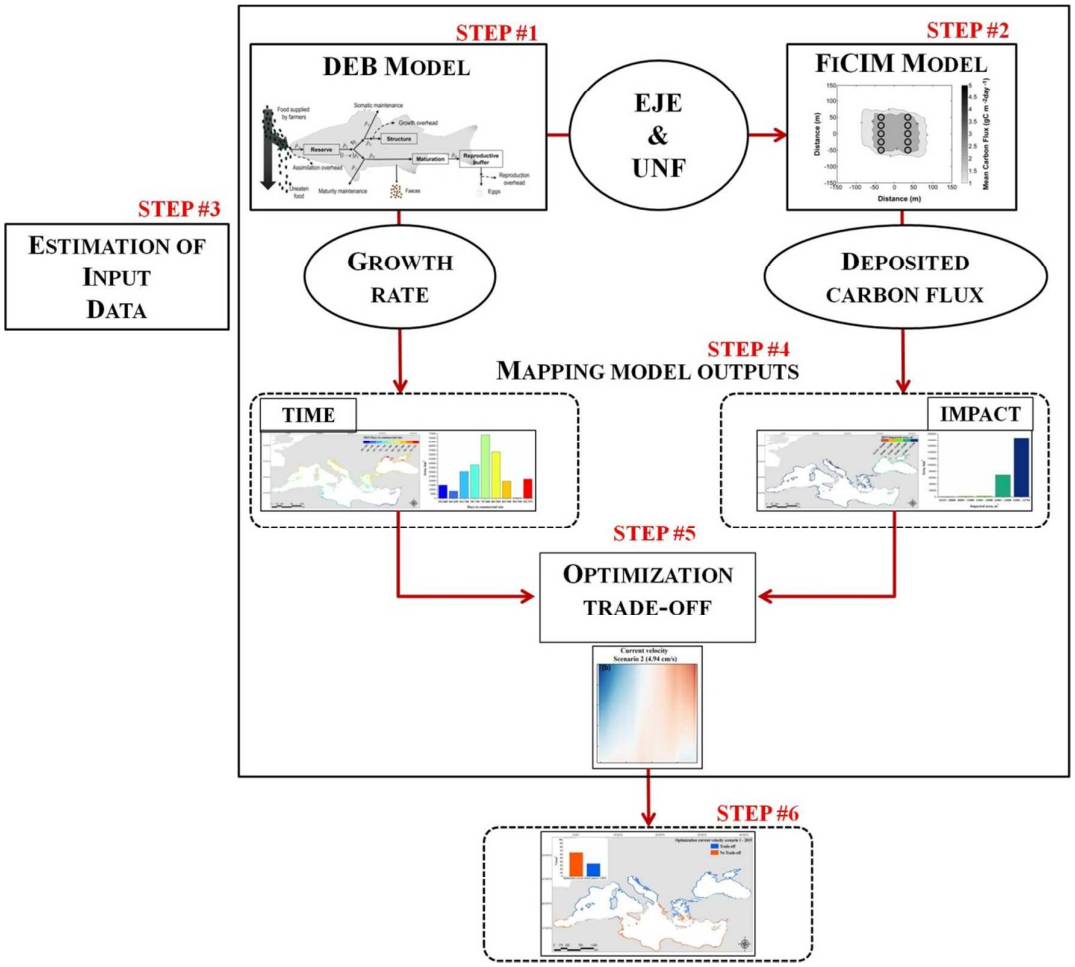
STEP #1
DEB MODEL
EJE
&
UNF
STEP #2
FICIM MODEL
STEP #3
ESTIMATION OF
INPUT
DATA
GROWTH
RATE
DEPOSITED
CARBON FLUX
STEP #4
MAPPING MODEL OUTPUTS
TIME
IMPACT
STEP #5
OPTIMIZATION
TRADE-OFF
STEP #6

Figure 1

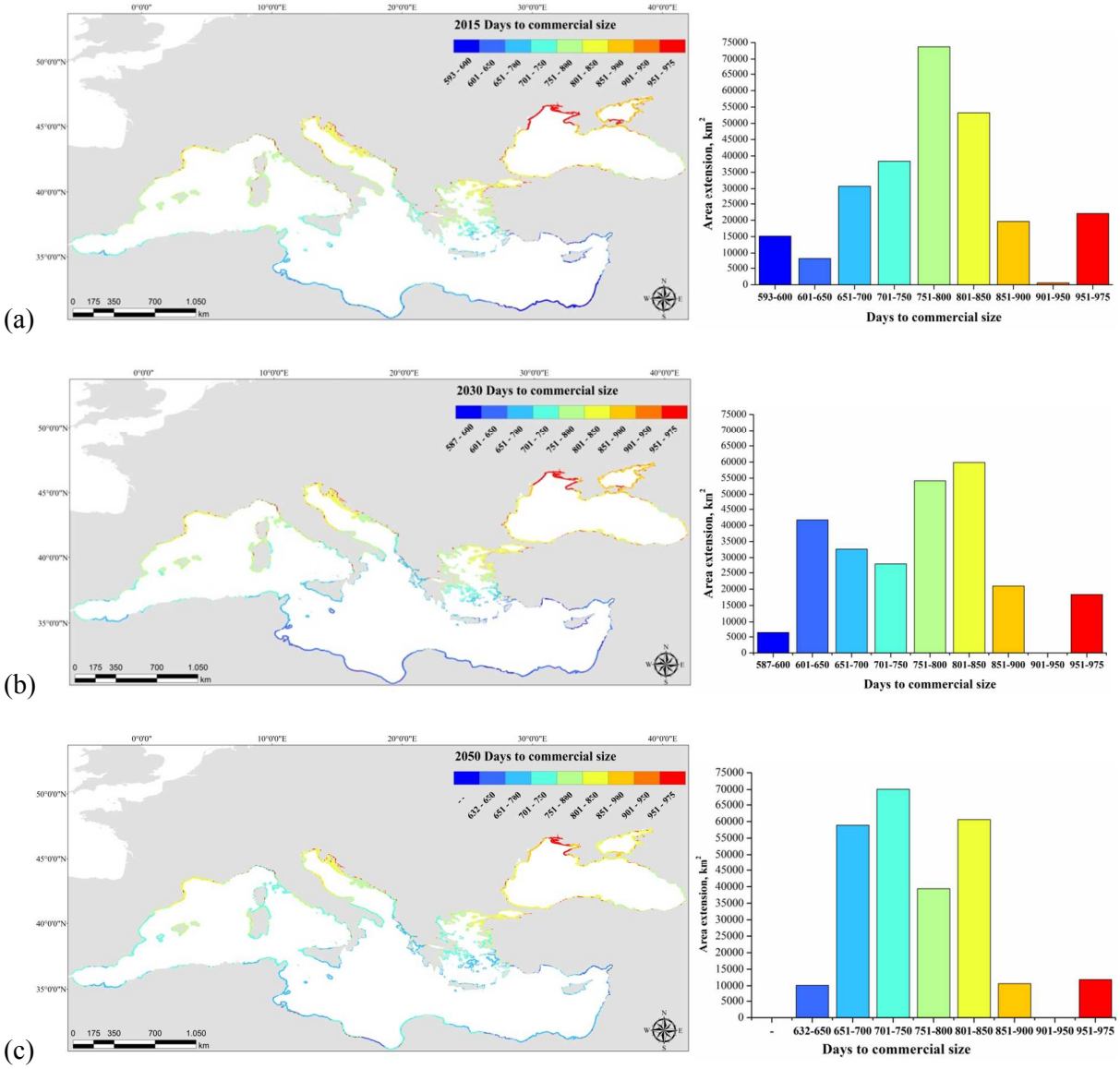
(a)
2015 Days to commercial size
593 - 600
601 - 650
651 - 700
701 - 750
751 - 800
801 - 850
851 - 900
901 - 950
951 - 975
0 175 350 700 1.050 km
Area extension, km²
Days to commercial size
593-600 601-650 651-700 701-750 751-800 801-850 851-900 901-950 951-975
(b)
2030 Days to commercial size
587 - 600
601 - 650
651 - 700
701 - 750
751 - 800
801 - 850
851 - 900
901 - 950
951 - 975
0 175 350 700 1.050 km
Area extension, km²
Days to commercial size
587-600 601-650 651-700 701-750 751-800 801-850 851-900 901-950 951-975
(c)
2050 Days to commercial size
632 - 650
651 - 700
701 - 750
751 - 800
801 - 850
851 - 900
901 - 950
951 - 975
0 175 350 700 1.050 km
Area extension, km²
Days to commercial size
- 632-650 651-700 701-750 751-800 801-850 851-900 901-950 951-975

Figure 2

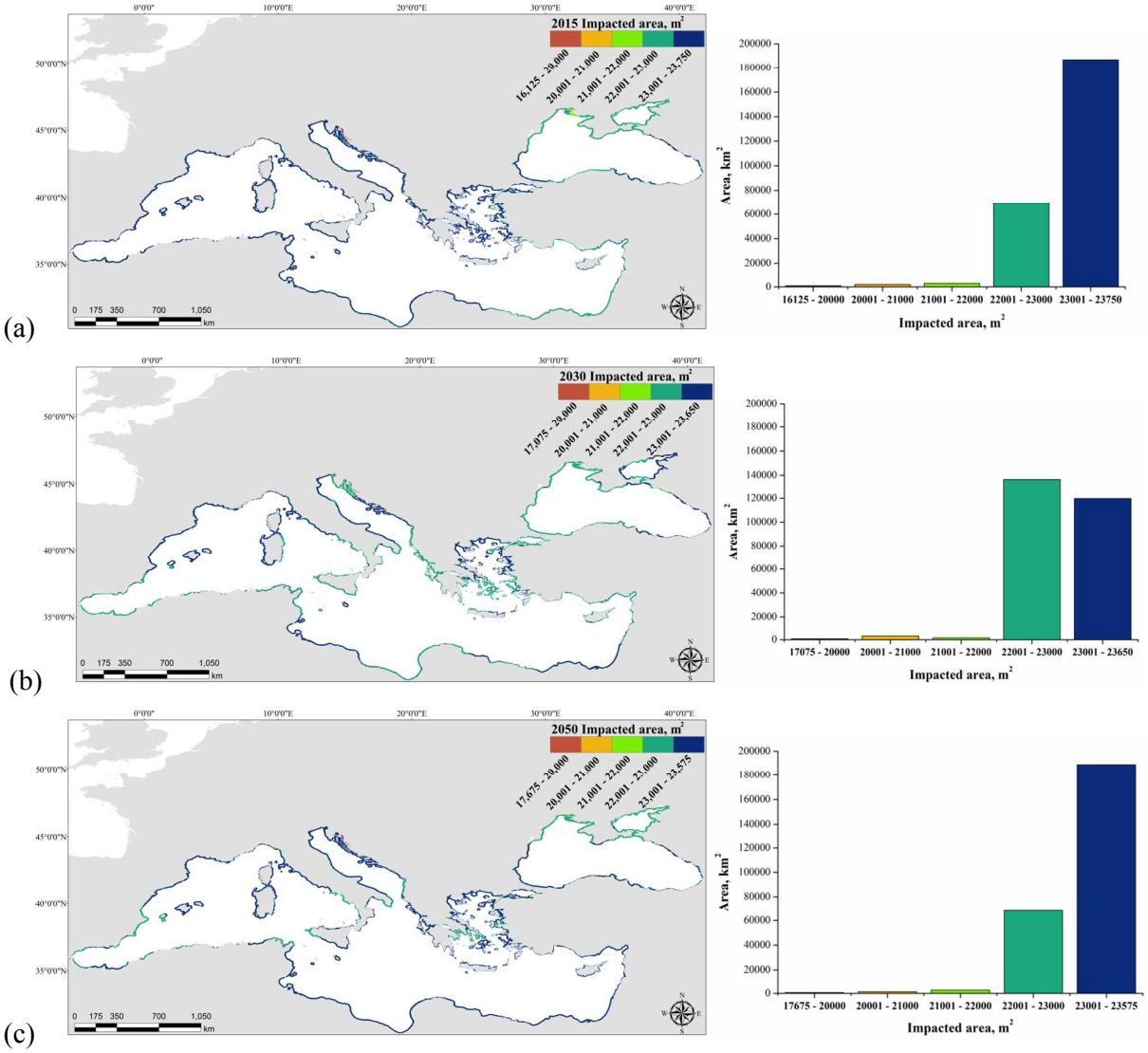
(a)
2015 Impacted area, m2
16,125 - 20,000
20,001 - 21,000
21,001 - 22,000
22,001 - 23,000
23,001 - 23,750
Area, km2
Impacted area, m2
16125 - 20000
20001 - 21000
21001 - 22000
22001 - 23000
23001 - 23750
(b)
2030 Impacted area, m2
17,075 - 20,000
20,001 - 21,000
21,001 - 22,000
22,001 - 23,000
23,001 - 23,650
Area, km2
Impacted area, m2
17075 - 20000
20001 - 21000
21001 - 22000
22001 - 23000
23001 - 23650
(c)
2050 Impacted area, m2
17,675 - 20,000
20,001 - 21,000
21,001 - 22,000
22,001 - 23,000
23,001 - 23,575
Area, km2
Impacted area, m2
17675 - 20000
20001 - 21000
21001 - 22000
22001 - 23000
23001 - 23575

Figure 3

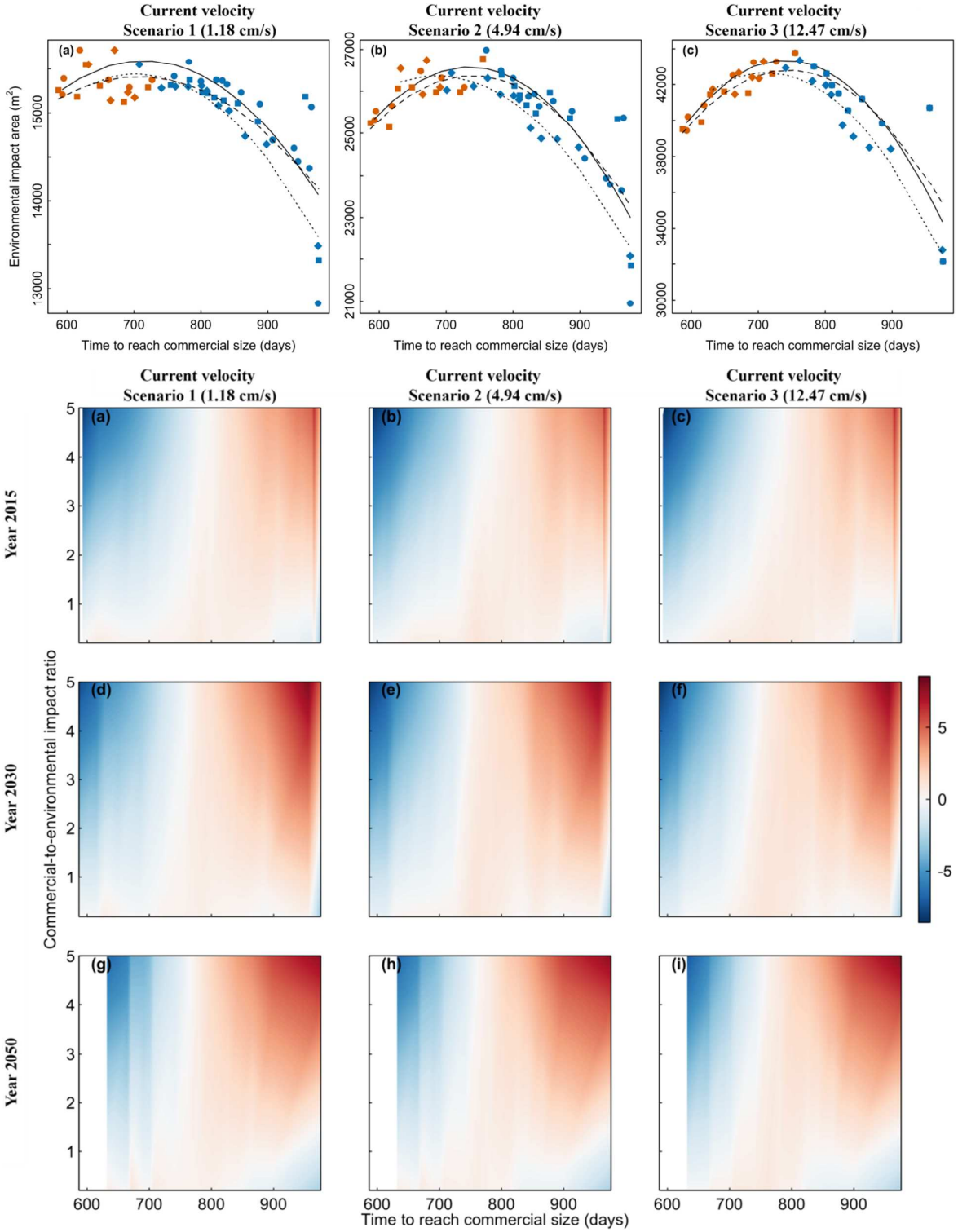
Current velocity
Scenario 1 (1.18 cm/s)
Current velocity
Scenario 2 (4.94 cm/s)
Current velocity
Scenario 3 (12.47 cm/s)
(a)
(b)
(c)
Environmental impact area (m²)
Time to reach commercial size (days)
Year 2015
Year 2030
Year 2050
Commercial-to-environmental impact ratio
(d)
(e)
(f)
(g)
(h)
(i)

Figure 4

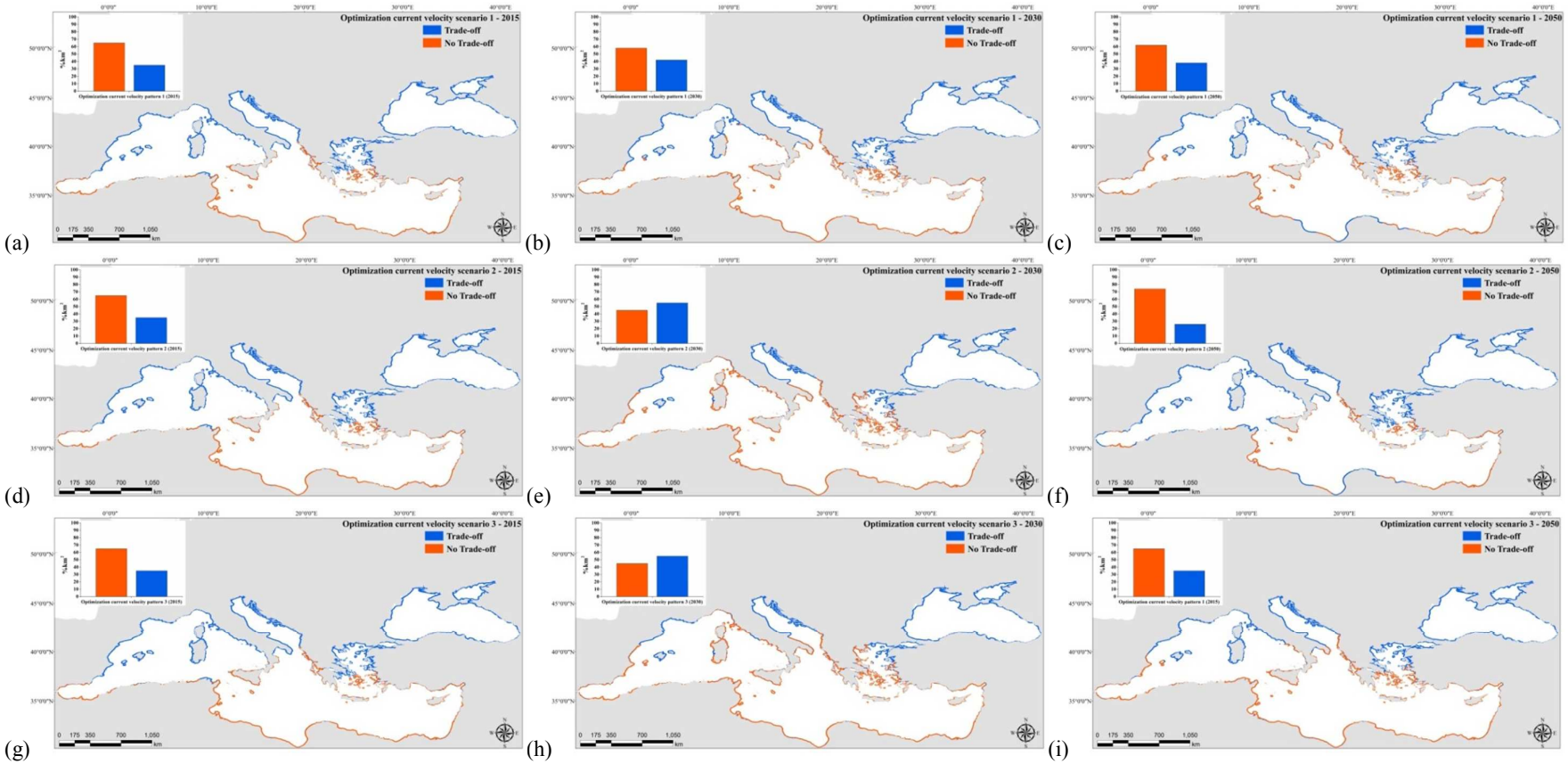
(a)
Optimization current velocity scenario 1 - 2015
Trade-off
No Trade-off
(b)
Optimization current velocity scenario 1 - 2030
Trade-off
No Trade-off
(c)
Optimization current velocity scenario 1 - 2050
Trade-off
No Trade-off
(d)
Optimization current velocity scenario 2 - 2015
Trade-off
No Trade-off
(e)
Optimization current velocity scenario 2 - 2030
Trade-off
No Trade-off
(f)
Optimization current velocity scenario 2 - 2050
Trade-off
No Trade-off
(g)
Optimization current velocity scenario 3 - 2015
Trade-off
No Trade-off
(h)
Optimization current velocity scenario 3 - 2030
Trade-off
No Trade-off
(i)
Optimization current velocity scenario 3 - 2050
Trade-off
No Trade-off

Figure 5